

**Figure 2.** Oxygen (1s) photopeak of film 4 (—), along with the best curve fit (---).

the other three films. The most striking feature in this micrograph is the formation of highly dispersed particles in the polymer matrix. Furthermore, these particles have a near uniform size distribution. The average particle size, in this micrograph as well as the other three, ranged between 20 and 80 nm. Also present in the TEMs is a depletion zone of 4.6  $\mu\text{m}$ . The loss of 5% of the dopant material alone cannot account for this depletion zone. Therefore this material is believed to have either formed atomically dispersed particulate matter that cannot be observed by TEM or has migrated from this area of the film. Upon examination of higher magnification TEM photos, it is difficult to distinguish phase contrast from surface and near-surface particulate matter. X-ray photoelectron spectroscopy (XPS) revealed evidence of a surface layer of iron oxide (vide infra) on the modified films. Up to 10 atom % iron was observed in the first 50 Å of the air-side surface. Thus supporting the theory of atomically dispersed particulate matter.

Figure 2 shows a typical oxygen(1s) photopeak obtained from the analysis of the iron-modified films. The top spectrum was generated from film 4. The curve fit of this spectrum is represented by the set of four bands shown as the bottom spectrum. Bands at 533.2, 532.3, and 531.6 eV<sup>4</sup> are assigned to the ether, ketone, and imide functionalities of the polyimide.<sup>5</sup> These oxygen functionalities have a relative concentration of 1:1:4, which is what is expected for a BTDA/ODA polyimide. The peak at 530.1 eV is assigned to an oxide oxygen. Similar binding energies have been reported for oxygen in various iron oxides.<sup>6</sup> The relative atomic concentrations of oxygen to iron in the four films ranged between 1.34 and 1.70, which corresponds to a stoichiometry of either  $\text{Fe}_2\text{O}_3$  or  $\text{Fe}_3\text{O}_4$ . The position and width of the iron(2p) photopeak was found to be independent of the oxidation state of the iron in model iron oxides.

X-ray powder diffraction was used to aid in the identification of the iron oxide contained in the polyimide matrix. Of the four films, only film 4 gave a substantial signal in the X-ray diffractogram. The two major reflections in the spectrum were at  $d$  spacings of 2.52 and 1.48 Å, which are indicative of either  $\gamma\text{-Fe}_2\text{O}_3$  or  $\text{Fe}_3\text{O}_4$ . The reflections used to confidently distinguish the two oxides,

as determined from authentic samples, were not observed in our samples due to the substantial background noise arising from the polymer matrix. However, it was observed from the X-ray diffraction pattern that reflections due to  $\text{FeO}$ ,  $\alpha\text{-Fe}_2\text{O}_3$ , or any iron oxyhydroxides were not present.

Magnetic measurements performed on the iron-modified films further suggest the transformation of the  $\text{Fe}(\text{acac})_3$  dopant to  $\gamma\text{-Fe}_2\text{O}_3$  or  $\text{Fe}_3\text{O}_4$ . The coercivities of the iron-modified films were between 105 and 130 Oe. These values are lower than most literature values for iron oxides used in magnetic applications; however, the iron oxide particles in our films were cubic while higher coercivities are indicative of needlelike particles.<sup>7</sup>

We also find that heating only  $\text{Fe}(\text{acac})_3$  to 300 °C in a dry air atmosphere produces  $\gamma\text{-Fe}_2\text{O}_3$  as determined by X-ray diffraction. Furthermore, thermal treatment of  $\text{Fe}_3\text{O}_4$  at 300 °C in dry air for 1 h also produces  $\gamma\text{-Fe}_2\text{O}_3$ . Therefore if  $\text{Fe}_3\text{O}_4$  was produced in the films it would readily be transformed to  $\gamma\text{-Fe}_2\text{O}_3$  during the last stage of the thermal imidization process. For these reasons it is believed that the iron oxide particles produced in the films are  $\gamma\text{-Fe}_2\text{O}_3$ .

**Acknowledgment.** We thank Allco Chemical Co. for providing the BTDA. We also thank Amspec Chemical Co. for providing the  $\text{Fe}(\text{acac})_3$ . We gratefully acknowledge financial assistance by the National Aeronautics and Space Administration.

(7) Ishikawa, T.; Matijevic, E. *Langmuir* 1988, 4, 26.

## Intercalation Chemistry of Layered $\text{FePS}_3$ . An Approach toward Insulating Magnets below 90 K

René Clement,\* Leticia Lomas, and  
Jean Paul Audiere

Laboratoire de Chimie Inorganique, CNRS URA 420  
Batiment 420, Université Paris Sud  
91405 Orsay Cedex, France

Received July 16, 1990

In recent years, considerable effort has been devoted to the synthesis of insulating, molecular-based materials exhibiting bulk ferro- or ferrimagnetism. However, most materials synthesized so far have very low Curie temperatures, typically in the range 1–15 K.<sup>1,2</sup> Very few exceptions occur, such as ammonium tetrachlorochromate(II), which orders ferromagnetically in the range 50–60 K.<sup>1</sup> This report describes a semiconducting intercalate in the  $\text{FePS}_3$  family, namely,  $\text{Fe}_{1-x}\text{PS}_3(\text{pyridinium})_{2x}(\text{solv})_y$  ( $x \approx 0.12$ ), which exhibits spontaneous magnetization below  $\approx 90$  K.

Transition-metal hexathiohypodiphosphates  $\text{MPS}_3$ , where M stands for a metal in the II+ oxidation state, form a family of lamellar materials, often described as broad-band semiconductors,<sup>3</sup> structurally similar to the well-known lamellar dichalcogenides (for a review see the article by Brec<sup>4</sup>). Several  $\text{MPS}_3$  compounds display a unique

(4) All photopeaks were referenced to the carbon (1s) peak at 284.6 eV, of the aromatic groups in the polymer backbone.

(5) Clark, D. T.; Thomas, H. R., *J. Polym. Sci.: Polym. Chem. Ed.* 1987, 20, 790.

(6) McIntyre, N. S.; Zetaruk, D. G., *Anal. Chem.* 1977, 49, 1521.

(1) Day, P. *Acc. Chem. Res.* 1979, 12, 236.

(2) Miller, J. S.; Epstein, A. J.; Reiff, W. M. *Acc. Chem. Res.* 1988, 21, 114 and references therein.

(3) Klingenberg, W.; Ott, R.; Hahn, H. Z. *Anorg. Allg. Chem.* 1973, 396, 271.

(4) Brec, R. *Solid State Ionics* 1986, 22, 3 and references therein.

reactivity, as they take up cations from a solution and discharge intralamellar  $M^{2+}$  cations into the solution.<sup>5</sup>  $MPS_3$  are best described as two-dimensional arrays of  $M^{2+}$  ions assembled by  $P_2S_6^{4-}$  bridging ligands, the M-S bonds still being quite labile.<sup>5</sup>

The magnetic properties of the  $MPS_3$  compounds have already been examined. The pure materials order antiferromagnetically<sup>6-8</sup> below a critical temperature (78 K for  $M = Mn$ , 120 K for  $M = Fe$ ). At higher temperatures, they are paramagnets with antiferromagnetic (AF) interactions.<sup>4</sup> In 1980, one of us showed that intercalating  $MnPS_3$  with various guest cations resulted in a dramatic modification of the magnetic properties:<sup>9</sup> whereas the behavior above the ordering temperature was still dominated by AF interactions, the intercalated material below the ordering temperature (33 K for the cobalticinium intercalate) exhibited spontaneous magnetization and a typical hysteresis loop. The magnetization at saturation was about 15% of the value expected if all the spins were aligned.<sup>10</sup>

The increasing importance of the "molecular ferromagnets" prompted us to reexamine the problem of achieving high ordering temperatures, and the following strategy was designed: (i) obtain an intercalate with a concentration of vacancies  $x$  as small as possible to reduce spin dilution effects; (ii) use  $FePS_3$  instead of  $MnPS_3$ , as the ordering temperature of the former is significantly higher.

The "cation exchange" intercalation chemistry of  $FePS_3$  has not been well developed yet, and the necessity to control the concentration of vacancies led us to look for new synthetic routes. Insertion of pyridine (py) into some  $MPS_3$  compounds has already been reported,<sup>11,12</sup> and indication has been found that in some cases  $M^{2+}$  ions ( $M = Mn, Cd$ ) were released from the lattice during the insertion process. This suggests that pyridinium ions ( $pyH^+$ ) are involved, and it is possible that an optimized reaction would take place if a ( $pyH^+$ , py) mixture was used instead of pure py.

It turns out that intercalation of  $FePS_3$  under these conditions can be readily achieved. In a typical experiment, 200 mg of  $FePS_3$  (ground powder) was treated with a solution of 1 g of  $pyH^+Cl^-$  and 1 g of py in 10 mL of water for 3 days at 50 °C under nitrogen atmosphere. The black powder obtained was then washed with water then ethanol, dried over silica gel, and then handled in air. No insertion occurs if the aqueous solution contains either the pyridinium salt or the pyridine alone.

Infrared spectroscopy shows evidence of the presence of some water (broad bands near 3500 and 1600  $cm^{-1}$ ) and of py or  $pyH^+$  species (main sharp bands at 1485, 1385, 737, 665  $cm^{-1}$ ); The  $\nu(PS_3)$  asymmetric stretching band, which occurs at 570  $cm^{-1}$  in pure  $FePS_3$ , is split into two components at 606 and 556  $cm^{-1}$ , as invariably observed in the  $MPS_3$  intercalates containing intralamellar metal vacancies.<sup>13</sup>

Table I. Indexation of  $Fe_{0.88}PS_3(pyH + py)_{0.36}(H_2O)_{\approx 0.5}$  at Room Temperature<sup>a</sup>

spacing, Å		<i>hkl</i>	intens
obsd	calcd		
9.725	9.720	001	s
5.180	5.180	020	w
4.864	4.860	002	w
3.240	3.240	003	m
2.930	2.931	130	s
2.771	2.771	200	m
2.661	2.661	131	m
2.311	2.311	132	m
2.087	2.087	202	m
1.726	1.726	060	s
1.700	1.700	061	s

<sup>a</sup> Cell dimensions:  $a = 6.001$  Å,  $b = 10.361$  Å,  $c = 10.527$ , and  $\beta = 112.60$  Å.

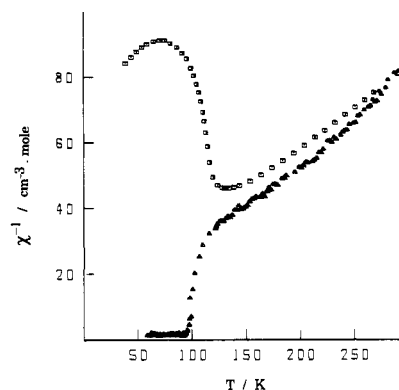


Figure 1. Reciprocal magnetic susceptibility (per mole of Fe) vs temperature of pure  $FePS_3$  ( $\square$ ) and of intercalate 1 ( $\triangle$ ). The molar susceptibility of 1 at 295 K is  $11.7 \times 10^{-3} cm^3 mol^{-1}$ .

Full insertion was ascertained by X-ray powder diffraction: samples partially intercalated appear as diphasic mixtures of pure  $FePS_3$  and of the intercalate. The latter appears to be well crystallized, as it exhibits sharp  $hkl$  reflections. These reflections could be readily indexed by using a monoclinic unit cell (Table I) closely related to that of pure  $FePS_3$ . Parameters  $a$  and  $b$  along the plane of the layers remain essentially unchanged. The interlamellar distance increases by  $\approx 3.3$  Å as a result of intercalation, thus demonstrating that the planes of the guest molecules lie parallel to the layers.

Elemental analyses of the material were obtained (% in weight: Fe, 23.2; P, 14.6; S, 45.4; C, 10.2; N, 2.1; H, 1.3). These data lead to the formula  $Fe_{0.88}PS_3(pyH + py)_{0.36}(H_2O)_{\approx 0.5}$  (1). A significant loss of  $Fe(II)$  cations accompanies the intercalation process, and therefore most of the organic guest species must be present as pyridinium to balance electrical charges. The amount of water, the presence of which is obvious from IR spectroscopy, is estimated by assuming an oxygen content such that the sum of the analysis figures is adjusted to 100%.

The temperature dependence of the reciprocal magnetic susceptibility  $1/\chi$  of material 1 (measured with a Faraday balance) is shown in Figure 1. Whereas pure  $FePS_3$  orders antiferromagnetically below  $\approx 120$  K, intercalate 1 undergoes a rather abrupt transition between 90 and 100 K. Above 100 K, the material is a paramagnet with AF exchange interactions. The  $\approx 135$  K susceptibility maximum of  $FePS_3$  is no longer observed on the curve of 1. This indicates that the AF exchange interaction between the iron spins is weakened in the intercalate, a feature in agreement with the existence of vacancies on the  $Fe^{2+}$  sublattice.

(5) (a) Clement, R. *J. Chem. Soc., Chem. Commun.* **1980**, 647. (b) Clement, R.; Garnier, O.; Jegoudez, J. *Inorg. Chem.* **1986**, *25*, 1404.

(6) Taylor, B. E.; Steger, J.; Wold, A. *J. Solid State Chem.* **1973**, *7*, 461.

(7) Kurowasa, K.; Saito, S.; Yamaguchi, Y. *J. Phys. Soc. Jpn.* **1983**, *52*, 3919.

(8) Jernberg, P.; Bjarman, S.; Wappling, R. *J. Magn. Magn. Mater.* **1984**, *46*, 178.

(9) Clement, R.; Girerd, J. J.; Morgenstern Badarau, I. *Inorg. Chem.* **1989**, *19*, 2852.

(10) Clement, R.; Audière, J. P.; Renard, J. P. *Rev. Chim. Miner.* **1982**, *19*, 560.

(11) Foot, P. J. S.; Shaker, N. G. *Mater. Res. Bull.* **1983**, *18*, 173.

(12) Cleary, D. A.; Groh, J.; Lifshitz, E.; Francis, A. H. *J. Phys. Chem.* **1988**, *92*, 55.

(13) Mathey, Y.; Clement, R.; Sourisseau, C.; Lucazeau, G. *Inorg. Chem.* **1982**, *6*, 2773.

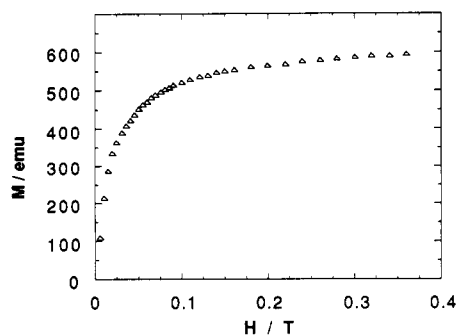


**Figure 2.** Magnetization (per mole of Fe) versus applied external magnetic field of intercalate 1, measured at 5 K.

Below 90 K, the magnetic susceptibility becomes very large, and field dependent but no longer temperature dependent. This suggests the onset in 1 of a magnetically ordered state associated with spontaneous magnetization. The following simple experiment is quite spectacular: when a Pyrex tube containing 1 is soaked in liquid nitrogen on top of a standard magnetic stirrer, the powder "flows" in the tube and follows the rotating rod; the phenomenon stops upon reheating.

Study of the magnetization  $M$  of material 1 as a function of the applied magnetic field has been carried out at 5 K using the Metronique Ingenierie SQUID magnetometer. Results are shown on Figure 2. The magnetization of the sample rapidly increases in low fields and then remains nearly constant in stronger fields. The saturation value of  $M$  (around 550 cgs emu/mol of iron) is only a fraction of the value expected ( $\sim 22000$  cgs emu/mol of Fe) if all spins were ordered parallel. These results may be interpreted in terms of the onset of weak ferromagnetism in material 1. This phenomenon arises from the canting of antiferromagnetically coupled spins in such a way that a net moment results. Alternatively, the spontaneous magnetization may also arise from uncompensated moments around the metal vacancies (which introduce some frustration) in the antiferromagnetic  $\text{Fe}^{2+}$  lattice.

The electrical conductivity of 1 along the layers plane was measured on a monocrystalline platelet between  $-50$  and  $+50$  °C by using a classical four-probe technique. The conductivity  $\sigma$  of 1 is very small ( $\sigma = 6.6 \times 10^{-7} \Omega^{-1} \text{cm}^{-1}$  at 25 °C) and thermally activated. A plot of  $\log \sigma$  versus  $1/T$  is linear and leads to an activation energy of  $\approx 0.2$  eV.

We note that syntheses carried out in the presence of a larger amount of pyridine result in a diphasic mixture consisting of material 1 and of a different  $\text{FePS}_3$  intercalate characterized by a basal spacing of  $\approx 12$  Å. We also note that long exposure ( $\approx 2$  weeks) of material 1 to air results in partial hydrolysis of the  $\text{P}_2\text{S}_6$  groups into phosphates (appearance of a broad IR band near  $1100 \text{ cm}^{-1}$ ).

The reason intercalation of the lattice results in such spectacular modification of the magnetic properties is not definitively understood, because of the impossibility of obtaining a detailed X-ray structure of this type of material. We have shown in the past that intercalation of  $\text{MnPS}_3$  causes local disorder and distortion around the metal, probably as a result of the creation of intralamellar vacancies that lower the local symmetry and introduce some frustration.<sup>14</sup> A better understanding of the role of intercalation is expected from EXAFS, Mossbauer, and neutron diffraction studies, which are currently in progress.

**Acknowledgment.** We thank E. Codjovi for his technical assistance.

## Preparation of Electrically Conducting Indium-Tin Oxide Thin Films by Heat Treatment of Mixed-Metal Hydroxide Dispersion Containing Polymer Binder

Takaki Kanbara, Masayuki Nagasaka, and Takakazu Yamamoto\*

Research Laboratory of Resources Utilization  
Tokyo Institute of Technology, 4259 Nagatsuta  
Midori-ku, Yokohama 227, Japan

Received May 30, 1990

ITO thin films are attractive materials for transparent electrodes and display panels, etc.,<sup>1</sup> and a variety of processes, such as vacuum evaporation,<sup>2</sup> radio frequency sputtering,<sup>3</sup> and spray pyrolysis<sup>4</sup> have been reported for the preparation of the ITO films. A more simple dip-dry-heat treatment method<sup>5-7</sup> has been also developed by using some organic compounds (e.g., alkoxide and acetylacetonate) of indium and tin. However, this method has not been applied to practical use since the pure organic compounds are relatively difficult to be prepared and expensive.

On the other hand, Woodhead and his co-worker reported that an indium hydroxide-tin hydroxide mixture highly dispersed in aqueous media (they called this dispersion system an aqueous sol/solution) gave a fine free-flowing ITO powder.<sup>8</sup> They also suggested usability of the aqueous sol/solution precursor as coating materials of metal wire and substrates. However, no report has been published on the usability of the aqueous sol/solution to prepare electrically conducting ITO thin film; this may be due to difficulty to prepare the electrically conducting ITO thin film because of aggregation of the metal hydroxide on substrate plates during the dip-dry process.

On the other hand, several kinds of water-soluble polymers, such as poly(vinyl alcohol) and (hydroxypropyl)cellulose, afford the indium hydroxide-tin hydroxide aqueous sol/solution with appropriate viscosity to prevent the aggregation of the metal hydroxide when added to the indium hydroxide-tin hydroxide aqueous sol/solution. The polymer binder can be easily removed by burning during firing of the indium hydroxide-tin hydroxide mixture. We now report preparation of the ITO thin films using the polymer-containing aqueous sol/solution.

Indium hydroxide-tin hydroxide mixture was first prepared by coprecipitation from an aqueous solution of  $\text{InCl}_3$  and  $\text{SnCl}_4$  (0–10% in  $\text{Sn}/(\text{Sn} + \text{In})$  atomic ratio); a dilute aqueous ammonia was added to the aqueous solution of  $\text{InCl}_3$  and  $\text{SnCl}_4$ . The resulting mixed hydroxide was washed with water repeatedly to remove  $\text{NH}_4\text{Cl}$  and collected by filtration.

The mixed hydroxide collected was then dispersed in water with vigorous stirring, and water-soluble polymer and dilute nitric acid were added to the hydroxide dispersion for preventing aggregation of the mixed hydroxide and controlling the pH of the dispersion systems (pH = 2–3),

(1) Kikuchi, I.; Ozawa, K. *Erekutoronikku Seramikusu* 1985, 5, 23.

(2) Mizuhashi, M. *Thin Solid Films* 1980, 70, 91.

(3) Itoyama, K. *Jpn. J. Appl. Phys.* 1978, 17, 1191.

(4) Kulaszewicz, S.; Jarmoc, W.; Lasocka, I.; Lasocki, Z. *Thin Solid Films* 1987, 148, L55.

(5) Furusaki, T.; Kodaira, K.; Yamamoto, M.; Shimada, S.; Matsushita, T. *Mater. Res. Bull.* 1986, 21, 803.

(6) Ogihara, S.; Kinugawa, K. *Yogyo Kyokaishi* 1982, 90, 157.

(7) Nomura, R.; Inazawa, S.; Matsuda, H.; Saeki, S. *Polyhedron* 1987, 6, 507.

(8) Woodhead, J. L.; Segal, D. J. *Br. Ceram. Proc.* 1985, 36, 123.

(14) Michalowicz, A.; Clement, R. *Inorg. Chem.* 1982, 21, 3872.